

Topological Defects in Spherical Nematics

Homin Shin, Mark J. Bowick, and Xiangjun Xing

Department of Physics, Syracuse University, Syracuse NY 13244-1130, USA

We study the organization of topological defects in a system of nematogens confined to the two-dimensional sphere (S^2). We first perform Monte Carlo simulations of a fluid system of hard rods (spherocylinders) living in the tangent plane of S^2 . The sphere is adiabatically compressed until we reach a jammed nematic state with maximum packing density. The nematic state exhibits four $+1/2$ disclinations arrayed on a great circle rather than at the vertices of a regular tetrahedron. This arises from the high elastic anisotropy of the system in which splay (K_1) is far softer than bending (K_3). We also introduce and study a lattice nematic model on S^2 with tunable elastic constants and map out the preferred defect locations as a function of elastic anisotropy. We establish the existence of a one-parameter family of degenerate ground states in the extreme splay-dominated limit $K_3/K_1 \rightarrow \infty$. Thus the global defect geometry is controllable by tuning the relative splay to bend modulus.

PACS numbers: 61.30.-v, 61.30.Jf, 02.40.-k

Ordered arrays of microscopic structures on curved interfaces provide a promising route to fabricating nanoscale or mesoscale building blocks (mesoatoms) that may in turn form molecules and bulk materials. One class of mesoatoms is provided by particles self-assembling on spherical droplets in liquid-liquid emulsions. The particles may be isotropic or shaped. Ordered structures on spherical interfaces always possess topological defects [1]. The location and detailed arrangement of such defects are both important since defects are distinctive regions which may be functionalized to create directional bonds akin to atomic bonds. This has been nicely illustrated recently by the synthesis of divalent gold nanoparticles coated with self-assembled stripes of phase-separated ligands whose two polar defects can be functionalized. The divalent nanoparticles subsequently link spontaneously to form chains [2].

Spherical nematics have a local 2-fold inversion symmetry and elementary disclinations of both half-integer and integer strength. Since the total disclination strength on the 2-sphere is two [3, 4], nematic ground states may possess four $+1/2$ defects, two $+1$ defects or two $+1/2$ s and one $+1$. Functionalization of the defects in the first case could lead to tetravalent mesoatoms with sp^3 -like directional bonding [3]. The structure and arrangement of defects in such a thin nematic shell with variable thickness has recently been studied both experimentally [5] and theoretically [6]. The analyses so far have, however, been limited to the one Frank constant approximation, in which the bending stiffness K_3 and the splay constant K_1 are equal [7]. Although fluctuations always drive these elastic moduli to the same value in the long wavelength limit, we are necessarily working at finite volume on the compact 2-sphere. It is essential, therefore, to explore the effect of differing bend and splay moduli on the structure of defects in the ground state.

To this end we have performed Monte Carlo simulations of hard rod fluids confined to the tangent plane

of the 2-sphere. Adiabatically shrinking the sphere increases the packing density and leads to a jammed state with nematic order and four $+1/2$ disclinations. Since like-sign defects repel, one might expect them to be maximally separated at the vertices of a regular tetrahedron [3, 4]. We find instead that the four defects lie approximately on a great circle. This can be understood as arising from the high bending stiffness K_3 compared to the splay stiffness constant K_1 . We also analyze a coarse-grained model of a spherical nematic with tunable Frank constants and map out the global pattern of defects as a function of the anisotropy K_3/K_1 . In the limit $K_3/K_1 \rightarrow \infty$, we show that the system exhibits a one-dimensional continuum of degenerate ground states in which the four defects form a rectangle of arbitrary aspect ratio.

Our Monte Carlo simulation is performed in the isobaric-isothermal (constant-NPT) ensemble with rod-like particles interacting via hard core repulsion [8]. We use spherocylinders with length L and diameter D (aspect ratio L/D). Isotropic initial states of N rods are prepared by centering each randomly oriented rod on a node of a spherical mesh of a 2-sphere of initial radius R_i . We perform $\sim 10^7$ Monte Carlo cycles, each of which consists of a translational and orientational trial move for all N rods together with a *volume-compression* move. The compression rate must be low enough to avoid premature jamming at low density. The simulation stops when the system is jammed and thus cannot be further compressed.

We simulated a system of $N = 1082$ rods with aspect ratio $L/D = 15$. The final radius reached was $R_f/D = 37.15$ starting from $R_i/D = 100$. The final states are found to be nematic with four $+1/2$ disclinations. This contrasts with the corresponding infinite system in 2D flat space where the densest packing state is crystalline [9]. At these system sizes, therefore, the spatial curvature of the surface frustrates crystalline or-

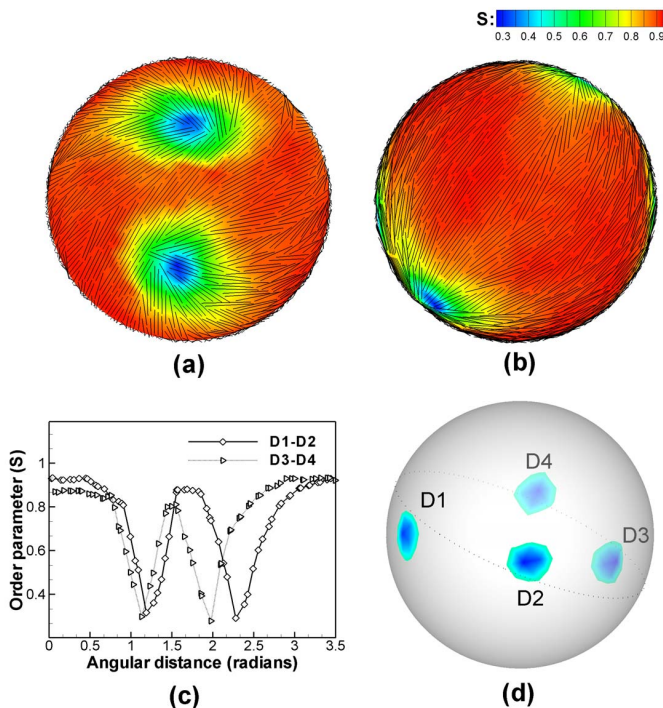


FIG. 1: (Color online) The ground-state configuration for spherical nematic ordering of 1082 rods with $L/D = 15$ is shown as the central lines of rods for clarity, together with maps of the local nematic order parameter. The two views are: (a) near defects and (b) nematic bulk. The radius of the compressed sphere is $R_f/D = 37.15$. The measurement of the order parameter along the great circle connecting defects is plotted as a function of angular distance in radians in (c). The exact locations of the four defects lying near one great circle are indicated in (d).

dering. Crystalline order is nevertheless expected to set in for larger system sizes, where the radius of curvature becomes much larger than the rod length. In simulations with short rods ($L/D < 7$) we find, in contrast, smectic-like domain structures at maximum density.

To characterize the nematic order we measure the local order parameter tensor $Q_{\alpha\beta}$, a symmetric, traceless second-rank tensor, by locally averaging the orientation of $m(V)$ rods $\hat{n}(a)$ within a small domain V (typically with an area of order L^2):

$$Q_{\alpha\beta} = \frac{1}{m(V)} \sum_{a \in V} \left(\hat{n}(a)_\alpha \hat{n}(a)_\beta - \frac{1}{2} \delta_{\alpha\beta} \right). \quad (1)$$

The nematic order parameter S is defined to be twice the positive eigenvalue of $Q_{\alpha\beta}$. Maps of S are shown in Figs. 1(a) and (b). The local order parameter along the great circle connecting the defects is also plotted versus angular distance in Fig. 1(c). The maximum value of S is about 0.93, in contrast with flat space where S reaches 1 [9]. The reduced maximum on the sphere results from the frustration due to the nonzero curvature enclosed in the region V . The defect cores are identified as the loci of

minima of the order parameter. Four $+1/2$ disclinations are clearly observed to lie on a single great circle, to within $\pm 0.15\text{rad}$, as illustrated in Fig. 1(d).

The planarity of the defect array can be explained by the strong elastic anisotropy. It is known that, for hard rod systems, the bend constant K_3 diverges as the rod density increases while the splay constant K_1 is almost independent of density [10, 11]. This leads to $K_3 \gg K_1$ at high packing density. To check this we determine the Frank constants by fitting the local director field surrounding a defect to a numerical minimization of the Frank free energy [12]. We find that $K_3/K_1 \gtrsim 20$.

Consider first planar nematics in the strong anisotropy limit. It is known that $+1$ disclinations admit both pure bending texture or pure splay texture [13, 14]. When the bending and splay constants are different one of these two textures will correspond to a minimum of the energy and the other a maximum. The energy of a $+1$ disclination is therefore given by $F^{(+1)} \sim \pi \min(K_1, K_3) \ln(R/a_0)$, where R is the system size and a_0 is the defect core size. The energy of a $+1/2$ defect, by contrast, depends on both K_1 and K_3 . In the one Frank constant limit $K_1 = K_3 = K$, the energy of a $+1/2$ disclination is one-quarter that of a $+1$ disclination: $F^{(+1/2)} \sim \frac{\pi K}{4} \ln(R/a_0)$. A $+1$ disclination will therefore unbind to a pair of $+1/2$ disclinations which may then separate. In the splay-dominated case $K_1 \ll K_3$, in contrast, the energy of $+1/2$ disclination is half that of a $+1$ disclination: $F^{(+1/2)} \sim \frac{\pi K_1}{2} \ln(R/a_0)$. Splitting a $+1$ defect therefore gains no energy and the total energy of two $+1/2$ disclinations is independent of their separation. All bending modes are frozen for a 2D nematic in flat space with $K_3 = \infty$. It can be shown in this limit that the integral curve of the director field is a geodesic (straight line). This implies that the 2D nematic director texture is completely determined by its configuration on a one-dimensional curve: there is no bulk degree of freedom that one can vary. In Fig. 2(a) we illustrate the formation and separation of a pair of $+1/2$ pure-splay defects by *global surgery* on a $+1$ pure-splay defect. The $+1$

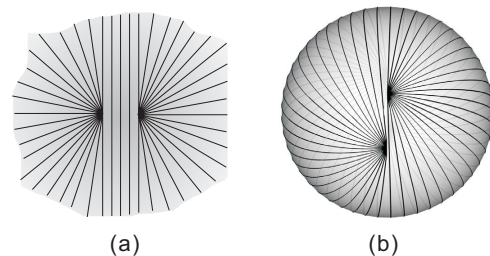


FIG. 2: (Color online) (a) In the limit of infinite K_3/K_1 , the separation of a $+1/2$ disclination pair in the plane costs no energy. (b) On the 2-sphere, an infinite number of states with four $+1/2$ disclinations on a great circle can be generated from a state with two $+1$ disclinations by cut-and-rotate surgery.

defect is pulled apart horizontally and the intermediate region filled with uniform nematic texture. Clearly it is also possible to pull apart the defect pair vertically without free energy cost. By contrast, any infinitesimal *local* deformation of the state in Fig. 2(a) generates bending deformations and is therefore forbidden energetically.

We now extend this argument to nematic order on the 2-sphere with infinite bending stiffness. The constraint of no bending again translates into the requirement that the integral curves of the director follow geodesic lines (great circles). Consider an initial state for which the director field follows lines of longitude everywhere. This state, with one +1 disclination at each pole, is clearly bending-free and is therefore a ground state in the limit $K_3 \rightarrow \infty$. Any local deformation of this state introduces bend and is therefore forbidden. There are, however, global manipulations that cost zero energy. As illustrated in Fig. 2(b), we can cut the sphere into two hemispheres along a great circle that contains both +1 disclinations, and rotate one hemisphere by an arbitrary angle α . This surgery divides each +1 disclination into two +1/2 disclinations and the resultant four +1/2 disclinations all lie on the great circle along which we cut. Note that the director field is everywhere smooth up to first order derivatives on the cut after the surgery [15], except at the disclination cores. The elastic free energy of the post-surgery state is therefore independent of the rotation angle α . We have thus identified a continuous manifold of degenerate low energy states, parameterized by the angle α , for spherical nematics in the pure-splay limit $K_3 \rightarrow \infty$. The energy difference between the four +1/2 disclination state and the original state with two +1 disclinations can only come from the defect core energies and these do not grow with radius R . It is thus negligible for large system sizes.

Starting from a pure splay state and rotating the director at every point by $\pi/2$ in the tangent plane, we obtain a pure bend state. It can also be shown that the splay and bending constants K_1 and K_3 interchange under this rotation. A system with $K_3/K_1 \ll 1$ should, therefore, also exhibit a similar one-parameter family of degenerate ground states with a co-planar configuration of defects. This is verified below. We note that the same cut-and-rotate surgery has been applied to spherical smectics (for which K_3/K_1 is also $\gg 1$) by Chantawansri et al; [16] and Blanc and Kleman [17].

To understand better how the global configuration of defects depends on the elastic anisotropy K_3/K_1 , we next analyze a lattice nematic model on S^2 in which the two Frank constants can be continuously varied. We first construct a triangular lattice on the 2-sphere with $N = 762$ vertices. As a result of the Gauss-Bonnet theorem, twelve of these vertices have coordination number five and form a regular icosahedron. It turns out, however, that these crystalline disclinations do not significantly affect the location of the nematic defects [18]. On every vertex a of this lattice we define a nematic director \hat{n}_a ,

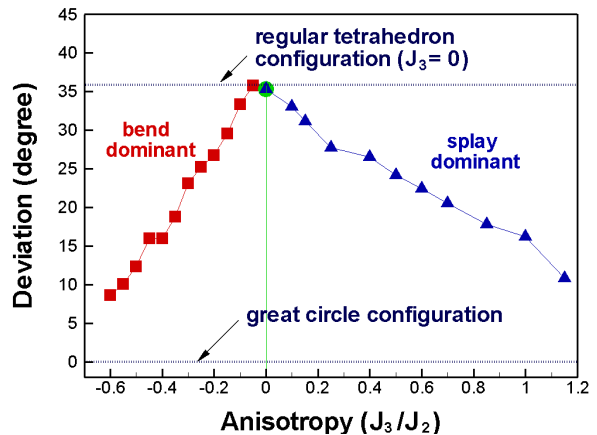


FIG. 3: (Color online) The effect of the anisotropy J_3/J_2 on the configuration of defects. As the anisotropy is turned on the defects shift from a tetrahedral geometry to a coplanar great circle alignment. The angular deviation of the defect positions from the great circle are measured as a function of the anisotropy.

which is constrained to the local tangent plane. The Hamiltonian is given by

$$H = J_2 \sum_{\langle a,b \rangle} \text{Tr}(N_a - N_b)(N_a - N_b) \quad (2)$$

$$+ J_3 \sum_{\langle a,b \neq c \rangle} (\hat{e}_{ab} \cdot N_a \cdot \hat{e}_{ac}) \text{Tr}(N_a - N_b) \cdot (N_a - N_c),$$

where N_a is the dyadic tensor $\hat{n}_a \hat{n}_a$, while \hat{e}_{ab} is the unit vector pointing from vertex a to vertex b . In Eq. (2) $\langle a,b \rangle$ means summation over all pairs of nearest-neighbor sites b and c that are both nearest neighbors of site a .

The lattice model Eq. (2) is manifestly invariant under spatial inversion of each director \hat{n}_a . The two body term with coefficient J_2 is precisely the 2D Maier-Saupe lattice model of nematics, which is known to reduce, at large scales, to the Frank free energy with equal elastic constants $K_1 = K_3$. The three body term with coefficient J_3 couples the directors explicitly to the underlying lattice and renders K_1 and K_3 different. It can be shown [19] that at large scales the lattice model Eq. (2) reduces to the following Frank free energy for spherical nematics:

$$F = \int \sqrt{g} d^2 \mathbf{r} \left[\frac{K_1}{2} (\vec{D} \cdot \hat{n})^2 + \frac{K_3}{2} (\vec{D} \cdot \hat{t})^2 \right], \quad (3)$$

where \vec{D} is the covariant derivative and \hat{t} is the unit tangent vector perpendicular to the director \hat{n} . We note that in going from Eq. (2) to Eq. (3), however, terms of higher order (in $D\hat{n}$) have been dropped. These terms, though irrelevant in the renormalization group sense, may be quantitatively important for small system sizes. The parameter J_3 in Eq. (2) turns out to be proportional to $(K_3 - K_1)/(K_3 + 2K_1)$. The coefficient of proportionality, however, depends on microscopic details [19].

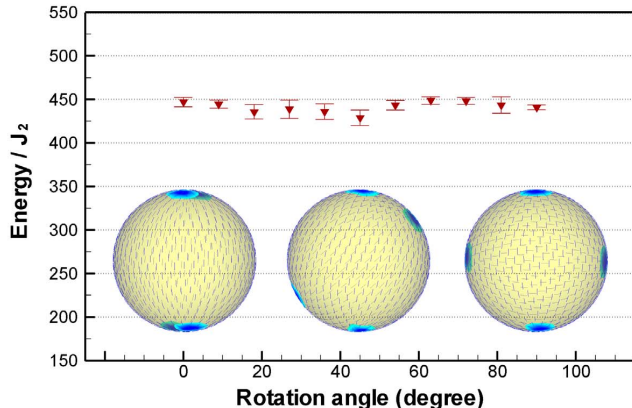


FIG. 4: (Color online) At $J_3/J_2 = 1.2$, the energy, as a function of the rotation angle α , is flat within $\pm 2\%$.

Starting from a random state, we determine the ground state of the model Eq. (2) using simulated annealing. We use the same method to identify the nematic defects as we used for the hard rods simulation. We first simulate the one Frank constant case for which $J_3 = 0$ and find that the four defects form a regular tetrahedron as expected [3, 4]. A non-zero three-body coupling J_3 leads to many metastable states. To avoid them, we start from the minimum energy configuration for the one Frank constant case and turn on the parameter J_3 at sufficiently low temperature. We then cool down again to reach the ground state. We find that the nematic texture becomes increasingly splay (bend) dominated as J_3 increases (decreases) from zero. We also measure the angular deviations of the defect locations from the circumscribed great circle, determined by a least squares fit. As shown in Fig. 3, the defects gradually shift toward a great circle as $|J_3|$ increases. When $J_3/J_2 \gtrsim 1.2$ or $\lesssim -0.6$, the director field develops a local instability, from which we infer that the splay or bend constant (at short scales) becomes negative. Nevertheless, the defect array is not strictly planar at $J_3/J_2 \approx 1.2$ or -0.6 . We suspect that this is due to the higher order terms that have been dropped in going from the discrete model Eq. (2) to the continuous model Eq. (3), which in principle can renormalize the two Frank constants and make them scale dependent. Such effects, however, are expected to diminish at large system sizes.

The lattice nematic model can be used to display explicitly the 1D manifold of degenerate ground states. For $J_3/J_2 = 1.2$, we start with a low energy state obtained by simulation of Eq. (2) in which the four defects lie approximately on the equator with an angular separation of 90° . We then force two defects to move within the great circle by rotating all the directors in the lower hemisphere. Starting from this new state we then minimize Eq. (2)

again at zero temperature. As shown in Fig. 4, the energy of all low energy states thus obtained, for different angular separation α , agree to within $\pm 2\%$. This small difference is likely due to finite size effects.

In this letter we have studied the global configuration of defects in the ground state of a spherical nematic using two different models. We show that the tetrahedral configuration crosses over to a *great-circle* configuration as we increase the anisotropy of the elastic constants. Our work therefore explicitly demonstrates that defect positions can be controlled by varying the elastic anisotropy. This result should be relevant to designing and fabricating mesoscopic molecules and bulk materials by attaching ligands to functionalized defect sites. The work of MJB and HS was supported by the NSF through Grants DMR-0219292 and DMR-0305407. The work of XX was supported by the American Chemical Society through Grant PRF 44689-G7. MJB thanks Robin Selinger for discussions.

-
- [1] D. R. Nelson, *Defects and Geometry in Condensed Matter Physics* (Cambridge University Press, Cambridge, 2002).
 - [2] G. A. DeVries *et al.*, *Science*, **315**, 358, (2007).
 - [3] D. R. Nelson, *Nano. Lett.* **2**, 1125 (2002).
 - [4] T. C. Lubensky, J. Prost, *J. Phys. II France* **2**, 371 (1992).
 - [5] A. Fernandez-Nieves *et al.*, *Phys. Rev. Lett.* **99**, 157801 (2007).
 - [6] V. Vitelli and D. R. Nelson, *Phys. Rev. E* **74**, 021711 (2006).
 - [7] G. Skacej and C. Zannoni, *Phys. Rev. Lett.* **100**, 197802 (2008).
 - [8] M. P. Allen and D. J. Tildesley, *Computer Simulation of Liquids* (Clarendon, Oxford, 1987).
 - [9] M. A. Bates and D. Frenkel, *J. Chem. Phys.* **112**, 10034 (2000).
 - [10] S.-D. Lee and R. B. Meyer, *J. Chem. Phys.* **84**, 3443 (1986).
 - [11] S.-D. Lee and R. B. Meyer, *Phys. Rev. Lett.* **61**, 2217 (1988).
 - [12] S. D. Hudson and E. L. Thomas, *Phys. Rev. Lett.* **62**, 1993 (1989).
 - [13] M. W. Deem, *Phys. Rev. E* **54**, 6441 (1996).
 - [14] Ref. [13] shows that negative-strength disclinations necessarily involve both bend and splay and therefore cost *infinite* energy in the strong anisotropy limit. Hence they don't appear in spherical nematic ground states and are not discussed further.
 - [15] Other cut-and-rotate manipulations either do not change the initial state or generate nematic director discontinuities, which are energetically costly.
 - [16] T. L. Chantawansri *et al.*, *Phys. Rev. E* **75**, 031802 (2007); A. Hexemer *et al.*, *Phys. Rev. E* **76**, 051604 (2007).
 - [17] C. Blanc and M. Kleman, *Eur. Phys. J. E* **4**, 241 (2001).
 - [18] We have also performed simulations on a random mesh on the 2-sphere and obtain similar results.
 - [19] H. Shin, M.J. Bowick and X. Xing, unpublished.